

Design of A Haptic Paddle for Accessible Integration of Data-Driven Methods in System Dynamics Education

Avinash Baskaran, Jamison Hood, Rhet O. Hailey *student member, IEEE*, and Chad G. Rose, *member, IEEE**

Abstract—Data-driven control, which embraces artificial intelligence, machine learning, and experience-based inferencing architectures, has gained significant interest for its ability to provide robust optimization in model-free, nonlinear, and time-varying paradigms. Traditional systems, such as the haptic paddle, used to communicate system dynamics principles in undergraduate curricula, have yet to be adapted to the memory and processing requirements of data-driven control. In this work, we present a modular, open-source 3D printable friction-driven haptic paddle design, building on the designs proposed by the community, using commercial components and simple microelectronic packaging, to enable robust data-driven control for integration in undergraduate education. We make use of the RP2040 microcontroller, a small light-weight logic platform capable of fast online computation and robust memory storage for onboard data-driven control. To validate our design, we first develop an experimental model of the physical dynamics that shows that our 3D printed friction drive is comparable with friction driven paddles and capstan-cable driven paddles. Further, we demonstrate the utility of our design in explicating data-driven control by presenting the development of basic machine learning and reinforcement learning architectures for online, model-free robust control in the presence of time-variable plant dynamics in a trajectory tracking task that is well suited for implementation in undergraduate and introductory graduate system dynamics and controls curricula.

I. INTRODUCTION

Undergraduate curricula in the area of Dynamics Systems and Control (DSC) are being developed to incorporate physical systems which exemplify theoretical principles and provide students with tangible expressions of theory [1]. When coupled with programmable microelectronics, physical systems offer students valuable insight and experience with practical engineering objectives. Multiple universities have extended the original design of the haptic paddle [2], such as the version presented here (Fig. 1) to provide hands-on experience in system dynamic characterization and control principles [3], [4], [5], [6]. Incorporation of such devices into the curriculum focused on experiential learning [7], [8] have been shown to have favorable outcomes in traditional academic metrics like oral and written examinations [9] in pre-, mid-, and post-class reflective assessments [10], application-oriented metrics including the technical quality and accuracy of written reports [11]. The haptic paddle can render common low-dimensional dynamics (e.g., mass-spring-damper dynamics) that are readily scaled and translated to industrial robotics applications [12], [13].

*This work was supported by the Council of University Transportation Centers (CUTC) New Initiatives Program.

The authors are with the Mechanical Engineering Department, Auburn University, Auburn, AL 36849 USA (e-mail: azb0180@auburn.edu).



Fig. 1. This paper presents an innovative design for the Auburn Haptic Paddle, which supports increased accessibility via 3D-printed and commercial-off-the-shelf components (CoTS) to facilitate the integration of data-driven control in system-dynamics education.

However, despite the success of the haptic paddle, a few drawbacks among its common versions inhibit further adoption and use in undergraduate curricula. Despite the wide-scale accessibility of tools needed to fabricate small-scale robotic systems, including 3D printers, many open-source haptic paddle transmission designs, including the popular cable-driven transmission, require high-accuracy fabrication methods such as laser cutting, to achieve high spatial resolution [4], [13]. Further, despite the development of increasingly ubiquitous microelectronic hardware and open-source integrated development support, many haptic paddles are outfitted with custom microelectronics packaging and software which are difficult to reproduce and limit the accessibility of the paddle to students and lay audiences [13]. Finally, existing haptic paddles make use of microcontrollers with extensive EEPROM memory. This architecture, while efficient, cost effective, and user-friendly, can impede the storage and access of recorded data required for data-driven approaches. With the development of more diverse microelectronic packaging having entered the market, these microcontrollers feature extensive Flash memory architectures which readily support on-board data-storage [14], [15].

This work presents an updated haptic paddle design to overcome limitations of current open-source designs. Critical drawbacks of contemporary haptic-paddle designs which impede their accessibility and adoption in engineering edu-

cation can be summarized as follows. Existing haptic paddle designs: 1. Rely on complex transmission designs [4], 2. Require either specific [4] or expensive [13] implementation hardware, and 3. Rely on microcontrollers that not well-suited to modern data-driven control approaches [14], [15].

In this work, we present an innovative haptic paddle design which uses: 1. Planar, modular design with a friction-driven transmission system that relaxes fabrication tolerances, 2. CoTS microelectronic hardware with a small physical footprint to facilitate easy fabrication, customization, and use, and 3. An RP2040 microcontroller with 2MB of Flash storage which supports robust data-logging and memory storage for data-driven control [16]. We explore the utility of this data logging feature in system characterization and learning-based control experiments. This paper presents the design and characterization of the Auburn Haptic Paddle, supporting low-cost fabrication, bandwidth competitive with high-fidelity paddle fabrication, and commercial-off-the-shelf hardware with memory-enabled microelectronics.

II. DESIGN OVERVIEW

A. Requirements

A haptic paddle supporting data-driven methods must have the ability to measure, store, and access meaningful training data and perform matrix calculations. These requirements can be segmented into analog-to-digital conversion (ADC), non-volatile (e.g., Flash) memory, RAM appropriate for the size and complexity of matrix calculations, efficient data access, a processor capable of efficiently performing matrix calculations, and/or the ability to interface with external processing units. Physical performance requirements include the ability to transmit forces to the user's hand with sufficient mechanical bandwidth (i.e. ≥ 10 Hz [4]), and render forces up to 5N without slipping [17]. Further, the total cost of the system should not exceed \$100 (compare with \$135, the cost of the leading alternative [4]).

In this section, we present developments to the hardware and microelectronic packaging to achieve these requirements. The Auburn Haptic Paddle (exploded views shown in Figs. 2 and 3) presented in this work is comprised of a DC motor which transmits torque to a rotating paddle via a friction interface. A magnet on the paddle handle generates a variable magnetic field which can be measured by a hall effect sensor. This system constitutes a single degree-of-freedom (DoF) interface with nonlinearities in the frequency and time domain as discussed further in Section III.

B. Transmission Design

The first major contribution is the development of a robust, easily assembled transmission design that can be fabricated using affordable 3D printers and provide high torque bandwidth and high-quality haptic inputs [19]. The uni-dimensional rotational motion of the Auburn Haptic Paddle lends itself to actuation by a DC motor, which can directly drive the paddle, or be amplified through a backlash-free transmission. Such transmission mechanisms are often favored as they allow for higher resolution motion

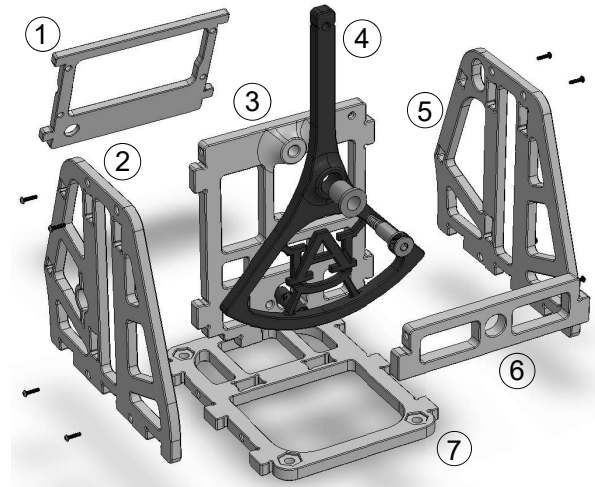


Fig. 2. The Auburn Haptic Paddle frame was designed to print quickly with key components including: (1) user interface mount, (2) left support, (3) main mounting plate, (4) paddle, (5) right support, (6) paddle support, and (7) base plate. Components (2), (3), and (5) are assembled using screws, and components (3) and (4) are assembled using shoulder bolts with a shaft collar. More details and instructions are available online [18]. Less modular conventional haptic paddle designs are visualized elsewhere [4] and can be compared with our modular approach.

control and torque amplification [13]. Among transmission mechanisms, cable-driven mechanisms have been a popular choice for haptic paddle implementations as they are robust to imperfections in the paddle structure that can arise from imprecise fabrication [4]. The cable is manually wound to ensure proper tension, and requires only two points of contact with the paddle on either side. However, cable-based transmission can be difficult to assemble and maintain, making them an inconvenient option for classroom use [4], [9], [11], [13]. Friction-driven mechanisms, by contrast, support simple and intuitive assembly. A disadvantage of friction-driven mechanisms is that they are more sensitive to imperfections in the paddle handle curved surfaces; however, modern 3D-printers can produce such curved surfaces with minimal artifacts and imperfections [19]. In Fig. 3, we illustrate our friction-based actuation strategy, in which a 12-volt DC motor fixed with a segment of CoTS rubber tubing on its shaft drives the paddle by rotating while pressed against the base of the paddle, adjustable by set screw.

C. Electronics

The second major contribution of this work is the introduction of a microelectronic architecture that supports convenient assembly and supply resiliency through modularity. The architecture features a CoTS logic board, power electronic packaging, and sensor assembled on our printed circuit board (PCB) [18] or assembled on a breadboard.

1) *Logic Board*: A critical feature of haptic platforms is the ability to simulate physical systems (e.g. mass-spring-dampers) realistically. To produce competitive, identifiable and effective haptic inputs to the hand, most haptic paddle designs make use of CoTS logic boards that can provide 1000 Hz bandwidth of closed loop feedback control (often

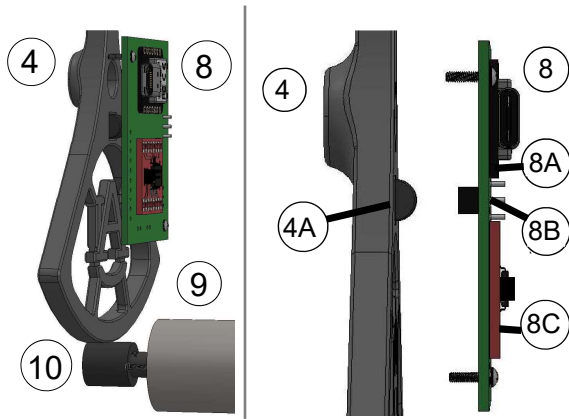


Fig. 3. The Auburn Haptic Paddle design features a friction-based transmission design (10), with a DC motor (9) and rubber tubing. The circuit board (8) houses a compact motor driver (8C) and a logic board (8A) for the hall effect sensor (8A), which measures the angular displacement of a small magnet (4A) mounted in the paddle handle.

packaged in a development board, like the Arduino Uno [4]. While the selection between different CoTS logic boards can be made according to convenience or familiarity, we desired a selection that maximizes control performance and capabilities in nonlinear, robust, and optimal approaches, especially in context of data-driven control. To accomplish this, we required a microcontroller with a high processing power and clock speed, large flash memory capacity, and robust analog and digital general purpose input-output (GPIO) and pulse width modulation (PWM) capabilities. To achieve these capabilities, we selected the RP2040 microcontroller [16].

Conventional microcontrollers and logic boards like Arduino platforms have limited flash storage capacity which is not conducive to data-driven methods and conventional Raspberry Pi platforms have large size and limited GPIO capabilities are inconsistent with the objective to minimize size, weight, cost, and power (SWaP-C) in the Auburn Haptic Paddle. The RP2040 microcontroller has gained much interest for small-scale robotics applications, due to its minimal SWaP-C footprint, large (2 MB) flash memory capacity supporting a wide variety of data-driven methods, and robust analog and digital GPIO capabilities. This is accomplished using dual-core ARM Cortex-M0+ processor core and nominal clock speeds of 133 mHz (higher than many conventional microcontrollers) supporting high processing speeds, accessible development capabilities via sufficient storage to support C++ and python (via a flash-able python interpreter), and UF2 USB-based bootloader to facilitate USB access facilitating transmission and reception of data. We further selected the Seeed Studio XIAO RP2040 logic board, which has a minimized size and GPIO footprint compared with other RP2040-based microcontrollers like the Raspberry Pi Pico, and which requires only 3.3 - 5.0 V, 2.0 mA input [16]. The RP2040 is one of the few widely available boards that satisfies the SWaP-C and memory requirements previously outlined in Section II-A.

2) *DC Motor and Motor Driver:* Next, we selected a DC motor and motor driver to drive the paddle. The DC motor specified in a common version of the haptic paddle [4] (Jameco PN 238473) was selected due to its minimal SWaP-C, high electromagnetic power density (lending to high torque capabilities), as well as its low rotor friction, inertia, and cogging torque. Many motor drivers for 12V motors are designing using bi-polar junction transistors (BJTs), which support high current loads and have lower cost and complexity in their construction. However, motor drivers constructed using metal-oxide-semiconductor field-effect transistor (MOSFETs) are increasingly considered for their numerous advantages, including high input impedance (i.e., low current consumption), higher switching speed and efficiency, support for higher voltage ranges, and better thermal efficiency. We selected the Toshiba TB6612FNG MOSFET-based H-bridge DC motor driver with low (5V) logic-level power requirements and sufficient output current (3.2 A intermittent).

3) *Sensor:* The sensor selected in our design represents a low SWaP-C electromagnetic transducer that is often used for position measurement in small-scale robotics applications and is functionally similar to the hall-effect sensor selected by other prominent haptic paddle platforms [4]. We selected the Allegro MicroSystems A1369EUA-24-T.

To provide students with an easy-to-use interface to the paddle software, which will allow them to select different control modes and tune control hyperparameters, our design features a user interface with an 2x16 I2C-based LCD screen, and an I2C potentiometer with detents enabling discrete physical selection modes. The wiring configuration for the user interface components is shown in Fig. 4 below. All microelectronic components of the Auburn Haptic Paddle can be readily purchased. The printed circuit mounting board can be purchased by sending the opensource CAD files to a commercial PCB manufacturer or replaced by a solderable breadboard for custom assembly. The total cost of all components in the Auburn Haptic Paddle including filament required for 3D printing is \$85.

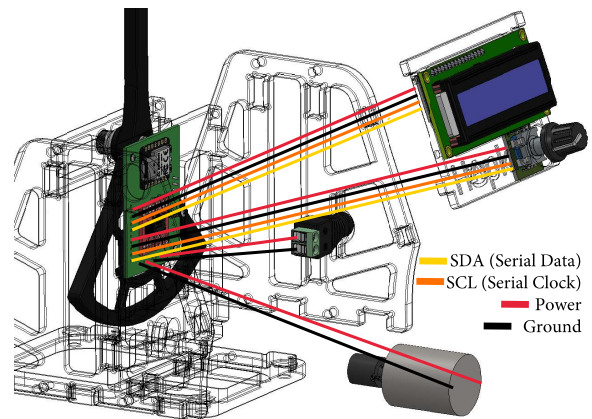


Fig. 4. Electronics layout and packaging in the Auburn Haptic Paddle

III. SYSTEM CHARACTERIZATION

The Auburn Haptic Paddle paddle can be readily modeled via analysis of its time- and frequency-domain dynamic characteristics. To characterize the frequency response of our haptic paddle, we passed multiple sine-waves at discrete frequencies from 1.5Hz to 20Hz as inputs to the motor driver (i.e., PWM commands transmitted to the DC motor), and recorded the position response of the paddle using the on-board position sensor. We then constructed a Bode magnitude plot, and estimated a model of the form: $\tau = I_{eq}\ddot{\theta} + b_{eq}\dot{\theta} + k_{eq}\theta$ using least squares estimation. We artificially imposed a spring constant in our control to ensure that the paddle returned to the center of the workspace (i.e. minimizing the physical drift of the paddle from its neutral position) [4]. Model parameters are reported in Table I, alongside the physical parameters of a similar device, Stanford University's HapKit 2.0 [4].

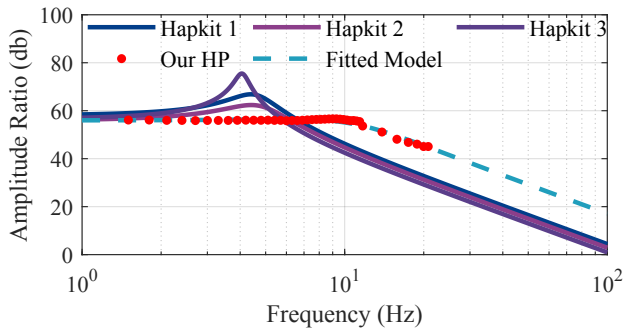


Fig. 5. A Bode plot of comparing common haptic paddle models with experimental characterization (red), and least-squares based model (blue dashed) is shown. Our design has higher bandwidth than similar alternatives due to the reduced mass of the paddle.

TABLE I

MODEL PARAMETERS OF HAPTIC PADDLE AND HAPKIT 2.0 [4].

Design	I_{eq} (Kgm ²)	b_{eq} ($\frac{Nm}{rad}$)	k_{eq} ($\frac{Nm}{rad}$)
Hapkit 2.0	1.82×10^{-6}	26.6×10^{-6}	15.9×10^{-4}
HAUptic Paddle	3.56×10^{-7}	27.8×10^{-6}	15.9×10^{-4}

The Stanford Univeristy Hapkit (versions 1, 2, and 3) was a key inspiration for our design. Versions 1 and 2 utilize friction drives, whereas version 3 utilizes a capstan drive which has been noted to be more difficult for users to assemble and debug. Our paddle has a higher position bandwidth due to reduced mass and resulting inertia of the paddle, which was designed to be thinner and lighter, taking advantage of developments in commercial 3D printers including robust temperature and force sensors, high-fidelity position control of servo motors, and reduced material costs to print thinner and lighter components with higher resolution, allowing reduction of the paddle inertia [19].

It was desired to characterize the friction drive transmission and to determine what loads would cause the paddle to slip. To accomplish this, a mechanical strain gauge was used to measured force applied to the paddle handle as shown in Fig. 6 while the paddle was set to initial displacements of -20, 10 0, 10, and 20 degrees from its upright resting position.

It was found that approximately 4.5N of force applied normal to the vertical plane would cause the paddle to slip at each starting angle.

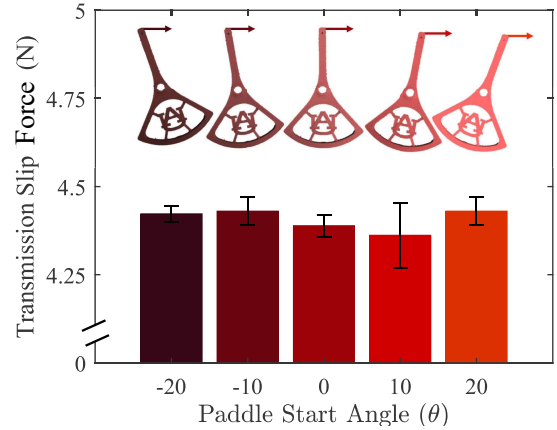


Fig. 6. Auburn HP transmission slip force (N) at standard starting angles.

IV. DATA-DRIVEN CONTROL DEMONSTRATION

We demonstrate the capabilities of the Auburn Haptic Paddle embedded system, which features robust memory storage and high computational bandwidth, in the context of data-driven approaches. Specifically, we selected a classical machine learning and reinforcement learning-based control demonstration which could be used to as an introductory project in a controls course [20].

A. Sample Task and Algorithm

To accomplish this, we designed a trajectory tracking task which can be readily ported as a workable example. The trajectory tracking task featured: 1.) Sim-to-real transfer of a feed-forward neural network (NN) - developed in MATLAB and trained on simulated data - to the physical system by exporting and storing pre-trained network weights on the microcontroller flash storage 2.) Implementation of data-driven model predictive control (DDMPC) which utilizes the trained network weights to generate and send control signals to the physical system online to track reference trajectories, and 3.) A basic reinforcement learning-based tuning of the NN in simulation using stochastic gradient descent (SGD) to handle time-variability in the plant model (i.e., sudden changes in the inertia, damping, and spring coefficients I_{eq} , b_{eq} , and k_{eq}). A schematic-level diagram of the trajectory tracking exercise is illustrated in Fig. 7, and summarized in Algorithm 1.

The algorithm describes the DDMPC development in MATLAB, which begins with initialization of actor network featuring a hidden layer with ten neurons. The actor network is pre-trained on a multi-sine position reference trajectory injected with gaussian noise. Then the actor is trained online using a stochastic gradient descent algorithm which optimizes the weights and biases of the neural network based on reward feedback. This system represents a low-level control-oriented reinforcement learning approach as the

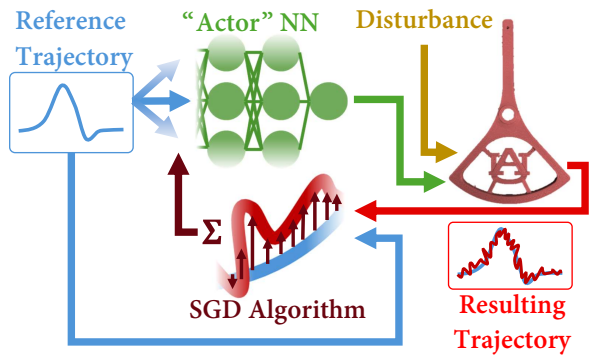


Fig. 7. A learning-based data-driven predictive control scheme for online trajectory tracking was developed to showcase the Auburn Haptic Paddle capabilities.

reward signal (position tracking error) is being used to update the actor as it acts on its environment (paddle simulation) [21]. More sophisticated RL approaches can be developed and implemented according to educational requirements.

Algorithm 1 Dynamic Data-driven Model Predictive Control with Stochastic Gradient Descent

- 1: Define transfer function coefficients a , b , and c
- 2: Define time parameters dt , t_{end} , and time vector t
- 3: Simulate noisy training data using multi-sine inputs
- 4: Split data into training and testing sets
- 5: Define and train an actor feedforward neural network
- 6: Define prediction horizon
- 7: Load desired trajectory
- 8: Define learning rate γ and number of iterations for SGD
- 9: **for** each iteration **do**
- 10: **for** each prediction horizon **do**
- 11: Extract desired trajectory for prediction horizon
- 12: Predict control inputs using neural network
- 13: Simulate system with predicted control input
- 14: Calculate MSE ($Loss$) of simulated trajectory
- 15: Compute $\nabla_{\theta} Loss$ wrt. network weights (θ)
- 16: Update network weights $\theta += -\gamma \nabla_{\theta} Loss$
- 17: **end for**
- 18: **end for**

B. Results

We characterize the performance of the Auburn Haptic Paddle in the data-driven control task of predicting and implementing torque outputs needed to track a desired trajectory in the machine learning and reinforcement learning paradigms. The NN, pre-trained on multi-sine data, was evaluated in simulation and in the physical system (Fig. 8) illustrates the performance of the pre-trained actor neural network (i.e., classical machine learning example).

Next, the agent was trained over 900 iterations with time-variable plant dynamics. on the first iteration, I_{eq} was tripled (fig 9 far left), on the 300th iteration b_{eq} was tripled (middle left), on the 600th iteration k_{eq} was increased by a factor of ten (middle right). The evolution from red to black

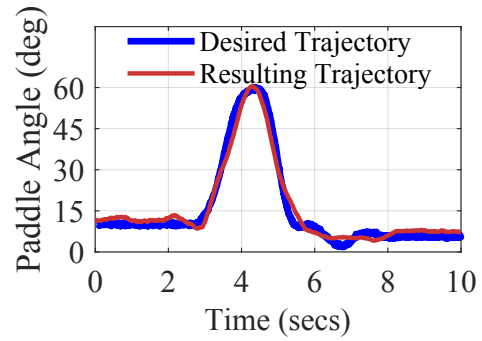


Fig. 8. Trajectory tracking performance on the physical haptic paddle demonstrating efficient and effective training and illustrating robust capabilities of the haptic paddle in data-driven control applications.

trajectories illustrate iterative convergence to the optimal actor network weights in each case. Then, to exemplify the capability of the optimized actor on the physical system, the trained optimized agent is implemented on the physical paddle where these altered dynamics were implemented artificially via resistive control effort to counteract the agent’s control effort. The results illustrate good performance of trained actors, congruence between the simulation and physical environment, and robust usability for students to develop innovative control designs to counteract disturbances.

TABLE II
PERFORMANCE OF SIMULATED (S) AND EXPERIMENTAL (E) MACHINE LEARNING (ML) AND REINFORCEMENT LEARNING (RL) ARCHITECTURES)

Condition	Approach			
	S. ML	E. ML	S. RL	E. RL
MAPE	5.44 %	6.05 %	6.55 %	9.36 %

The resulting trajectory generated by the agent in simulated and experimental machine learning (S. ML and E. ML) schemes yielded 5.44 % and 6.05 % mean absolute percentage error (MAPE), and the simulated and experimental reinforcement learning (S. RL and E.RL) schemes yielded 6.55% and 9.36% MAPE respectively.

V. DISCUSSION

Taken together, the data-driven frequency domain system modeling, reliable simulation environmental, and experimental data-driven control (all code available on Github [18]) indicate that the Auburn Haptic Paddle is well modeled and readily amenable to data-driven control approaches. Despite the success of the Auburn Haptic Paddle in supporting reliable and robust data-driven control in a low-cost, high-bandwidth platform, there are several drawbacks in our design and implementation. While fully 3D printable, the design can take up to 5 hours to print with reliable speed and accuracy settings on nominal commercial 3D printers [19]. Further, while all components are CoTS, their indefinite commercial availability from manufacturers is not guaranteed, such that continual updates to the design to support CoTS available components is necessary. Finally, while our Github repository includes robust device documentation for

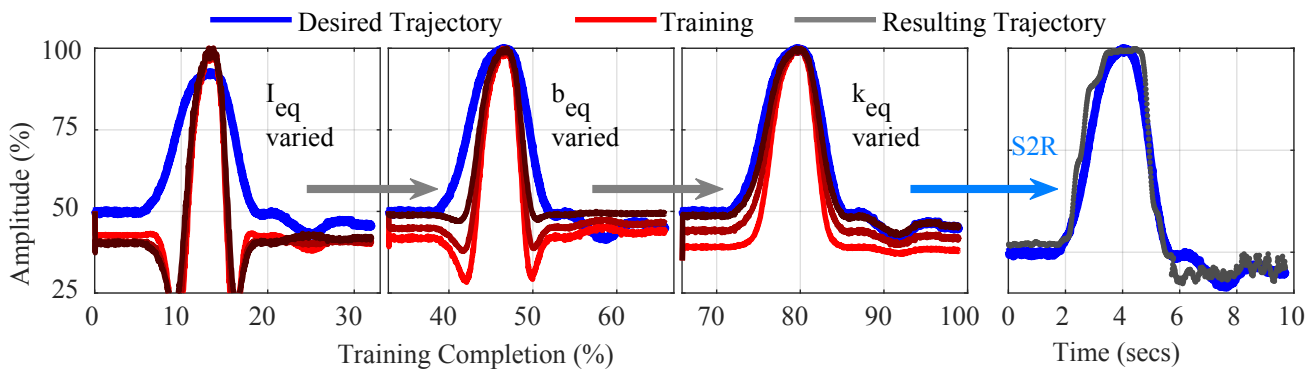


Fig. 9. The actor neural network was tuned in an RL scheme to time-variability in the plant dynamics. This is exemplified when I_{eq} was tripled (fig 9, b_{eq} was tripled, and k_{eq} was increased by a factor of ten at three different points during RL tuning of the pre-trained network. The trained actor was implemented on the paddle with the varied dynamics. Results indicate that the trained actor network is able to stabilize the MPC control dynamics in simulation and practice under diverse dynamics.

assembly, programming, and troubleshooting, effort remains to establish reliable materials for integration of the Auburn Haptic Paddle into system dynamics curricula, including expanded workable exercises for faculty and students, support for high-fidelity characterization (i.e., attachment points for digital multimeters and oscilloscopes), and experimental characterization of learning outcomes in the classroom [9].

VI. CONCLUSIONS

In this work, we propose fundamental advancements to the state of the art in design and fabrication of the haptic paddle, an educational platform which has been, and continues to be successfully employed to improve system dynamics curricula by providing students with a physical system. We expand on prior work by optimizing the design of the paddle for efficient 3D printing and assembly and sourced CoTS microelectronics which can be readily assembled on the open-source PCB design we provide or a soldered breadboard. We exemplify innovative approaches in data-driven control including reinforcement learning and model predictive control using the advanced memory capabilities of the latest RP2040 microcontroller. We exemplify model-free trajectory-based haptic guidance in various dynamic conditions, an archetypal case of data-driven control, to empower students not only with the ability to produce data-driven control systems but to experience them in a hands-on paradigm. Together, these capabilities provide students and educators with an integrated platform for data-driven DSC education.

ACKNOWLEDGMENT

The authors sincerely thank Chandler Stubbs and Zack Miller for assistance with design work. The authors gratefully acknowledge Dr. Larry Rilett's collaboration and the CUTC funding on the project, aimed at outreach and education in human-robot interaction in transportation.

REFERENCES

- [1] M. Berland and U. Wilensky, "Comparing virtual and physical robotics environments for supporting complex systems and computational thinking," *J. of Science Ed. and Tech.*, vol. 24, pp. 628–647, 2015.
- [2] C. Richard, A. M. Okamura, and M. R. Cutkosky, "Getting a feel for dynamics: Using haptic interface kits for teaching dynamics and controls," in *ASME International Mechanical Engineering Congress and Exposition*, vol. 18244, pp. 153–157, ASME, 1997.
- [3] M. O. Martinez *et al.*, "3-d printed haptic devices for educational applications," in *2016 IEEE Haptics Symposium*, pp. 126–133, 2016.
- [4] M. Orta Martinez *et al.*, "Evolution and analysis of hapkit: An open-source haptic device for educational applications," *IEEE Transactions on Haptics*, vol. 13, no. 2, pp. 354–367, 2020.
- [5] R. B. Gillespie, M. Hoffinan, and J. Freudenberg, "Haptic interface for hands-on instruction in system dynamics and embedded control," in *HAPTICS*, pp. 410–415, IEEE, 2003.
- [6] Zulqarnain, M. H. Koul, and I. Shahdad, "Towards an open source haptic kit to teach basic stem concepts," in *Proceedings of the 2017 3rd International Conference on Advances in Robotics, AIR '17*, New York, NY, USA: Association for Computing Machinery, 2017.
- [7] D. A. Kolb, *Experiential learning: Experience as the source of learning and development*. FT press, 2014.
- [8] C. S. E. Jamison *et al.*, "Experiential learning implementation in undergraduate engineering education: a systematic search and review," *European J. of Eng. Ed.*, vol. 47, no. 6, pp. 1356–1379, 2022.
- [9] R. Gassert *et al.*, "Physical student–robot interaction with the ethz haptic paddle," *IEEE Trans. on Ed.*, vol. 56, no. 1, pp. 9–17, 2012.
- [10] C. G. Rose *et al.*, "Reflection on system dynamics principles improves student performance in haptic paddle labs," *IEEE Transactions on Education*, vol. 61, no. 3, pp. 245–252, 2018.
- [11] J. L. Gorlewicz *et al.*, "A formal assessment of the haptic paddle laboratories in teaching system dynamics," in *2012 ASEE Annual Conference & Exposition*, no. 10.18260/1-2–20809, June 2012.
- [12] J. Hrbček *et al.*, "Control system for the haptic paddle used in mobile robotics," *International Journal of Advanced Robotic Systems*, vol. 14, no. 5, p. 1729881417737039, 2017.
- [13] C. G. Rose, J. A. French, and M. K. O'Malley, "Design and characterization of a haptic paddle for dynamics education," in *2014 IEEE Haptics Symposium (HAPTICS)*, pp. 265–270, 2014.
- [14] N. Dey and A. Mukherjee, *Embedded systems and robotics with open source tools*. CRC press, 2018.
- [15] R. B. Reese and B. A. Jones, "Improving the effectiveness of microcontroller education," in *Proceedings of the IEEE SoutheastCon 2010 (SoutheastCon)*, pp. 172–175, IEEE, 2010.
- [16] "Getting started with Seeed Studio XIAO SAMD21," wiki.seeedstudio.com/Seeeduino-XIAO, 2022. Accessed 1/23.
- [17] L. T. Gwilliam, A. J. Doxon, and W. R. Provancher, "Haptic matching of directional force and skin stretch feedback cues," in *2013 World Haptics Conference (WHC)*, pp. 19–24, IEEE, 2013.
- [18] "Auburn University Haptic Paddle GitHub Repository," <https://github.com/WeBRLab/hAUPtic-paddle>. Accessed 2/23.
- [19] A. J. Lopes *et al.*, "Comparison of ranking models to evaluate desktop 3d printers in a growing market," *Additive Manufacturing*, vol. 35, p. 101291, 2020.
- [20] J. Frochte *et al.*, "Seamless integration of machine learning contents in mechatronics curricula," in *2018 19th Intl. Conf. on Research and Ed. in Mechatronics*, pp. 75–80, IEEE, 2018.
- [21] L. Baird *et al.*, "Gradient descent for general reinforcement learning," *Advances in neural information processing systems*, vol. 11, 1998.